

Phase Behavior and Morphological Studies of Polyimide/PVP/Solvent/Water Systems by Phase Inversion

JONG HAK KIM,^{1,2} BYOUNG RYUL MIN,² HYUN CHAE PARK,¹ JONGOK WON,¹ YONG SOO KANG¹

¹ Center for Facilitated Transport Membranes, Korea Institute of Science and Technology, P.O. Box 131, Cheongryang, Seoul 130-650, South Korea

² Department of Chemical Engineering, Yonsei University, Seoul 120-749, South Korea

Received 13 July 2000; accepted 11 November 2000

ABSTRACT: The solubility gaps for poly(vinyl pyrrolidone) (PVP) in four polyimide solutions (NMP, DMF, GBL, DMSO) were determined by cloud point measurement and correlated with $\chi_{PI/Solvent}$ and $\Delta\delta_{PVP/Solvent}$. Membranes prepared with NMP and DMF systems showed a tendency of suppressing fingerlike structure with addition of PVP. On the other hand, membranes prepared with GBL and DMSO systems showed an inclination toward inducing macrovoid formation. These effects of PVP on the membrane morphology were explained by means of miscibility gap, viscosity of the polymer solution, polymer–polymer phase separation, and overall porosity. © 2001 John Wiley & Sons, Inc. *J Appl Polym Sci* 81: 3481–3488, 2001

Key words: polyimide (PI); PVP; phase inversion; macrovoid; phase separation

INTRODUCTION

Most asymmetric membranes used commercially are fabricated by immersion precipitation technique.¹ During immersion precipitation, liquid–liquid phase separation proceeds in a polymer solution until the porous structure is fixed by vitrification of a polymer-rich phase. The phase-separation behavior of membrane-forming systems plays a crucial role in determining the membrane morphology and its performance.^{2,3}

Addition of a third component to the casting solution, consisting of a polymer and a solvent, is a widely used method to control membrane morphology. Water-soluble polymers such as polyvinylpyrrolidone (PVP),⁴ polyethyleneglycol (PEG),⁵ inor-

ganic salts,⁶ surfactants,⁷ and both nonsolvent⁸ and solvent additives^{9–11} have been commonly used as a third component.

The roles of additives in the structures of membranes are dependent on the system used. Several researchers have reported that the addition of a third component into a dope solution could induce or suppress macrovoid formation in asymmetric membranes. Smolders et al.¹² demonstrated that the addition of water promoted macrovoid formation in the system of cellulose acetate/acetone/water with delayed demixing, while suppressing it in the system of cellulose acetate/1,4 dioxane/water with instantaneous demixing. Wang et al.⁷ reported that the addition of surfactants in the casting solution could induce or suppress macrovoids, depending on the miscibility between the added surfactant and the coagulant. Lai et al.⁸ also found that macrovoid formation could be suppressed or induced, depending on the content of nonsolvent additives such as *n*-butanol and cyclohexanol. In this study, the roles of PVP, which can

Correspondence to: Y. S. Kang (yskang@kist.re.kr).
Contract grant sponsor: Korean Ministry of Science and Technology.

Journal of Applied Polymer Science, Vol. 81, 3481–3488 (2001)
© 2001 John Wiley & Sons, Inc.

suppress or induce macrovoid formation, will be studied in polyimide (PI) systems with varying solvents in a pure water coagulant and interpreted in terms of the miscibility gap, the viscosity of the polymer solution, polymer–polymer phase separation, and overall porosity.

EXPERIMENTAL

Materials

The polyimide (PI) used was Matrimid 5218, supplied by Ciba-Geigy Co. (Summit, NJ). Its M_w and M_n were 80,000 and 46,000, respectively, characterized by GPC. The solvents were dimethylformamide (DMF; Junsei), *N*-methyl-2-pyrrolidinone (NMP; Aldrich Chemicals, Milwaukee, WI), γ -butyrolactone (GBL; Aldrich), and dimethylsulfoxide (DMSO; Aldrich). Distilled water was used as a coagulant. Polyvinylpyrrolidone (PVP, M_w 40,000; Polysciences, Warrington, PA) was used as a polymer additive. All chemicals were used without further purification.

Cloud Point Measurement

A series of polymer solutions with 15 wt % of PI concentration were prepared in vials with Teflon-lined cap. Different amounts of PVP and water were added to the PI solutions and PI/PVP solutions, respectively. The solutions were then mixed in a shaking water bath for 1 to 2 days at elevated temperature (60–80°C) until the complete dissolution was obtained. Thereafter, the solutions were cooled to 25°C and the cloud points were observed visually. In particular, the concentration of PVP making the PI solution turbid was adopted as the solubility gap of PVP.

Viscosities of Dilute Solutions

Dilute solution viscosities of PI and solvents were measured with a Ubbelohde viscometer at 22°C. The precision in efflux times was ± 0.1 s and temperature was maintained at 22 ± 0.05 °C.

$$\eta_{red} = \frac{\eta_{sp}}{C} = [\eta] + k'[\eta]^2C \quad (1)$$

$$\eta_{inh} = \frac{\ln \eta_r}{C} = [\eta] + k''[\eta]^2C \quad (2)$$

On the basis of eqs. (1) and (2), intrinsic viscosity, k' (Huggins constant), and k'' (Kraemer constant) were evaluated. Generally, k' is 0.35–0.4 and $k' - k''$ is about 0.5 for a good solvent. The values of k' and $k' - k''$ decrease and intrinsic viscosities increase as solvent power (affinity of polymer/solvent) increases.¹³

Light Transmittance Measurement

In studying the precipitation kinetics during the immersion precipitation process, the light transmittance method was employed.² The light transmittance curves as a function of time were obtained.

Membrane Preparation

Asymmetric PI membranes were prepared by a wet-phase inversion process. Polymer solutions were cast uniformly on a glass plate with a 200- μ m doctor blade and immediately immersed into a coagulation bath at 8°C. Membranes were kept in a nonsolvent bath for 1 day, dried in air, and then characterized. All membrane formation was conducted at 30–40% relative humidity and room temperature.

Overall Porosity

An overall porosity can be estimated with the area (A), the mass (W_m), the thickness (D) of membranes, and the density (ρ_p) of the polymer.⁸ After membranes were dried in air for 48 h and put in vacuum oven at 25°C for 48 h, the mass and the thickness were measured with an electronic balance and a thickness gauge as well as SEM. The percentage porosity was calculated as follows:

$$\begin{aligned} \text{Porosity (\%)} &= \frac{V_m - V_p}{V_m} \\ &\times 100 = \frac{DA - (W_m/\rho_p)}{DA} \times 100 \quad (3) \end{aligned}$$

Morphology

The cross-sectional morphologies of membranes were examined by scanning electron microscope (SEM; Hitachi model S-2500, Japan) after being fractured in liquid nitrogen and coated with gold.

RESULTS AND DISCUSSION

Thermodynamics of PI/PVP/Solvent Systems

The term PVP solubility gap represents a measure of the amount of PVP causing the phase

Table I Solubility Gap for PVP, $\Delta\delta_{\text{PVP/Solvent}}$ and $\chi_{\text{PI/Solvent}}$ of PI 15 wt % Solution at 25°C

System	Solubility Gap (%)	$\Delta\delta_{\text{PVP/Solvent}}^a$	$\chi_{\text{PI/Solvent}}$
PI/DMSO	2.0	4.05	0.49
PI/GBL	4.0	3.25	0.46
PI/DMF	13.0	2.25	0.32
PI/NMP	20.0 \uparrow	0.55	0.23

^a From Van Krevelen.¹³

separation of polymer solutions. In Table I, the solubility gaps for PVP in four PI solutions, $\chi_{\text{PI/Solvent}}$ and $\Delta\delta_{\text{PVP/Solvent}}$ are presented. χ of PI/solvent was determined from the activity coefficient by the UNIFAC method.^{14,15} However, $\Delta\delta$ was used instead of χ in the PVP/solvent pair because of unobtainable group contribution parameters of PVP. Although the solubility of PI and PVP in four solvents and the compatibilities between PVP and PI are excellent¹⁶ (solubilities of two polymers in four solvents were more than 20 wt %, according to our measurement), the addition of small amounts of PVP in PI/DMSO and PI/GBL solutions induced phase separation, that is, a PI-rich phase and a PVP-rich phase. It is well known that the phase separation polymer1/polymer2/solvent systems is ascribed to polymer-polymer phase separation, that is, a polymer1-rich (polymer2-lean) phase and a polymer2-rich (polymer1-lean) phase.¹⁶ The low solubility gaps for PVP in PI/DMSO and PI/GBL solutions can be explained in terms of the low affinities of DMSO and GBL to both PI and PVP (high $\chi_{\text{PI/DMSO}}$, $\chi_{\text{PI/GBL}}$ and high $\Delta\delta_{\text{PVP/DMSO}}$, $\Delta\delta_{\text{PVP/GBL}}$), whereas the high solubility gap for PVP in the PI/NMP solution can be explained in terms of the high interactions of PI/NMP and PVP/NMP. The solvent power for PI was also confirmed by the dilute solution viscosities, as shown in Table II; that is, DMSO and GBL have poorer solvency than NMP and DMF for PI.

Table II Viscosities of Dilute PI Solution with Ubbelohde Viscometer at 22°C

System	$[\eta]$	k'	$k' - k''$
PI/DMSO	0.50	0.35	0.51
PI/GBL	0.48	0.39	0.50
PI/DMF	0.61	0.39	0.45
PI/NMP	0.67	0.34	0.49

Table III Binary Interaction Parameters

System	Interaction Parameter		
Water(1)/NMP(2)/ PI(3)/PVP(4)	$\chi_{12} = 1.0$ $\chi_{14} = 0.5$	$\chi_{13} = 2.3$ $\chi_{24} = 0.5$	$\chi_{23} = 0.23$ $\chi_{34} = -1.5$
Water(1)/DMF(2)/ PI(3)/PVP(4)	$\chi_{12} = 0.6$ $\chi_{14} = 0.5$	$\chi_{13} = 2.3$ $\chi_{24} = 0.55$	$\chi_{23} = 0.32$ $\chi_{34} = -1.5$

Virtual Binodals for PI/PVP/Solvent/Water Systems

The concept of virtual binodal, proposed by Boom et al.,⁴ is obtained by considering that the two polymers do not move relatively to each other during the first moments of phase inversion, if the molecular weights of polymers are sufficiently high. In this study, the virtual binodal was adopted to investigate the thermodynamics of quaternary systems. First, to construct the virtual binodal curves, the binary interaction parameters of each component need to be identified and those for the NMP and DMF systems are listed in Table III. The values of χ_{12} (solvent/water) in the NMP and DMF systems were obtained from VLE data and by taking the volume fraction of water as 0.5.^{18,19} χ_{13} (water/PI) and χ_{23} (solvent/PI) were taken from swelling equilibrium and the UNIFAC method,^{14,15} respectively. According to the osmotic pressure experiment by Boom's group, χ_{14} (water/PVP) and χ_{24} (NMP/PVP) were 0.48 ± 0.05 and 0.52 ± 0.05 , respectively.²⁰ Boom used both χ_{14} and χ_{24} as 0.5. Because it is known that the χ_{24} and χ_{34} values do not essentially influence the virtual binodal curves,²¹ we estimated both χ_{24} (DMF/PVP) and χ_{34} (PI/PVP). DMF is a rather poor solvent for PVP, compared with NMP on the basis of difference of solubility parameter.¹³ Thus, χ_{24} (DMF/PVP) was assumed to be 0.55. χ_{34} (PI/PVP) was also assumed to be -1.5, as it is reported that PI has better miscibility than PES for PVP₁₆ and the value of χ_{34} (PES/PVP) was -1.0 according to the study of Boom. The methods and procedures for calculating the virtual binodal composition were introduced by Boom et al.²¹

Membrane Morphology

The morphology results shown in Figures 1 and 2 indicate that addition of PVP in the casting solution can induce or suppress macrovoids, depend-

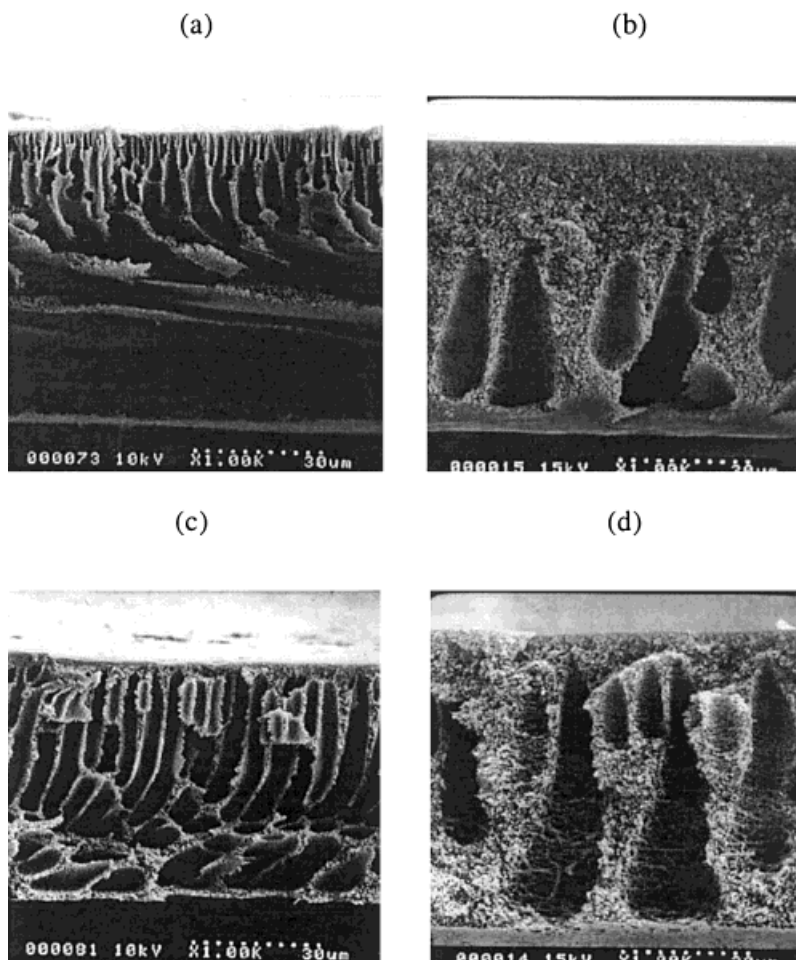


Figure 1 Suppression of macrovoid formation with addition of PVP: (a) PI/NMP = 15/85 wt %; (b) PI/PVP/NMP = 15/10/75 wt %; (c) PI/DMF = 15/85 wt %; (d) PI/PVP/DMF = 15/10/75 wt %.

ing on the systems. In NMP and DMF systems without PVP, the typical fingerlike structure was obtained. These membrane morphologies could be understood by considering that these systems had high affinities of NMP/water,¹⁸ DMF/water,¹⁹ and good solvency of NMP or DMF for PI. As described before, NMP and DMF are good solvents for PI in contrast to GBL and DMSO, according to our dilute solution viscosities. The addition of 10 wt % PVP into PI/NMP or PI/DMF solutions suppressed the finger formation. On the other hand, the spongelike structures were observed in GBL and DMSO systems without PVP. The spongelike structure in the GBL system may be the result of low interactions of GBL/water²² and GBL/PI. The mechanism of unexpected spongelike morphology in the DMSO system was analyzed in our previous study, in which we concluded that the characteristic thermodynamic features of the PI/

DMSO/water system might inhibit phase separation from proceeding further, thus undergoing insufficient liquid–liquid phase separation, which would induce the spongelike structure.¹⁵ The addition of 3 and 1 wt % PVP into PI/GBL and PI/DMSO solutions, respectively, induced macrovoid formation.

These phenomena, that the addition of PVP has opposite effects on membrane morphology, are investigated thermodynamically. Virtual binodal theory proposed by Boom's group²¹ was adapted only for the NMP and DMF systems because the phase separation takes place rapidly and, consequently, the polymer–polymer phase separation hardly occurs during the phase-inversion process. This seems to be the result of high affinities of solvent/water and solvent/polymer. In NMP and DMF systems, as the amount of PVP in polymer solutions increases, the miscibility gap

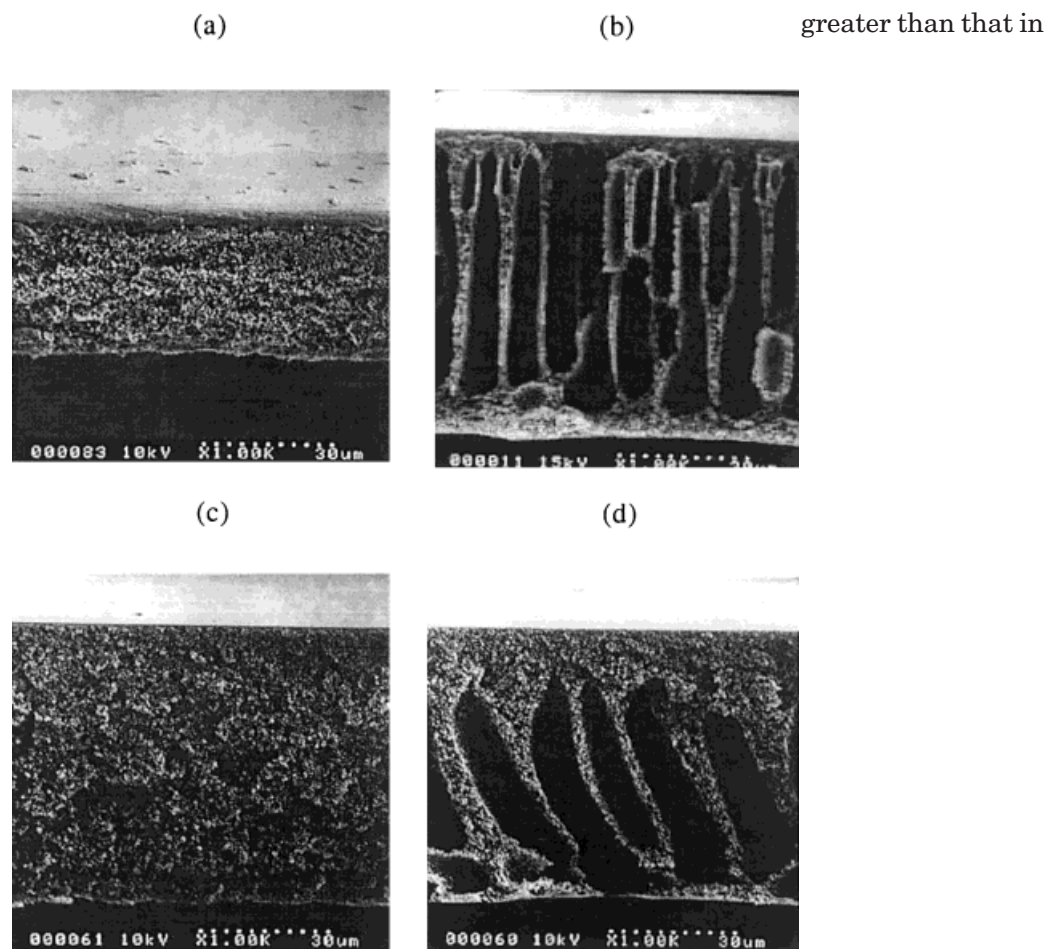


Figure 2 Promotion of macrovoid formation with addition of PVP: (a) PI/GBL = 15/85 wt %; (b) PI/PVP/GBL = 15/3/82 wt %; (c) PI/DMSO = 15/85 wt %; (d) PI/PVP/DMSO = 15/1/84 wt %.

applied by the virtual binodal theory grows larger (Figs. 3 and 4). When the polymeric additive with a high enough molecular weight is added, the enlargement of the miscibility gap implies the suppression of macrovoid formation.⁴ In addition, the kinetics of the phase separation supports the thermodynamics according to light transmittance. In Figure 5 the addition of 10 wt % PVP into the PI/NMP solution slows down the precipitation rate, which may be caused by the increase of the polymer solution viscosity. It is generally accepted that the increase of the solution viscosity prohibits the fingerlike structure.²³ Conclusively, the suppression of fingerlike structure by addition of PVP into NMP and DMF systems would be comprehended in terms of both the enlarged miscibility gap thermodynamically and the increased polymer solution viscosity.

When the NMP system is compared with the DMF system, the degree of reduction of macro-

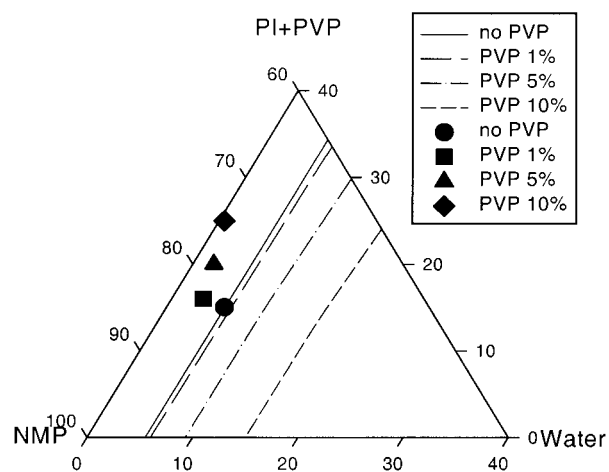


Figure 3 Cloud points and virtual binodal curves in the PI/PVP/NMP/water system. The lines are calculated virtual binodal and points are experimental cloud points.

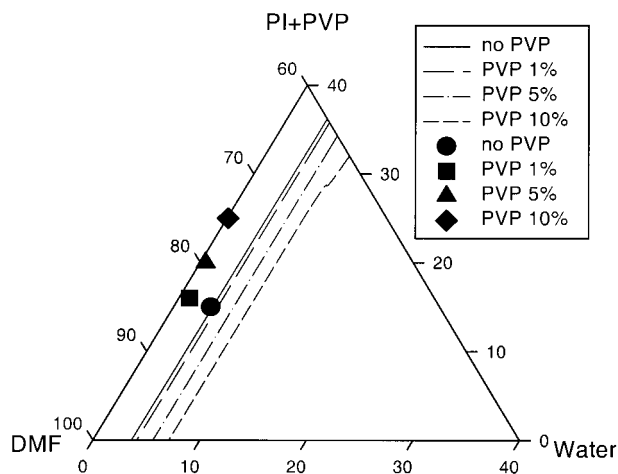


Figure 4 Cloud points and virtual binodal curves in the PI/PVP/DMF/water system. The lines are calculated virtual binodal and points are experimental cloud points.

the DMF system with the same amount of PVP (10 wt %; Fig. 1). This inclination is consistent with the results of virtual binodal curves. PVP 10 wt % allowed the polymer solution to contain about 18 wt % of water in the NMP system (Fig. 3) but about 8 wt % of water in the DMF system (Fig. 4). In addition, the degree of the real binodal shift in the DMF system was more excessive than that in the NMP system, although the trend that binodal curves in both systems shift to a polymer–solvent axis was similar with increasing amounts of PVP.

Again, we can quantitatively determine the degree of shift in binodal curve (DSBC) as follows:

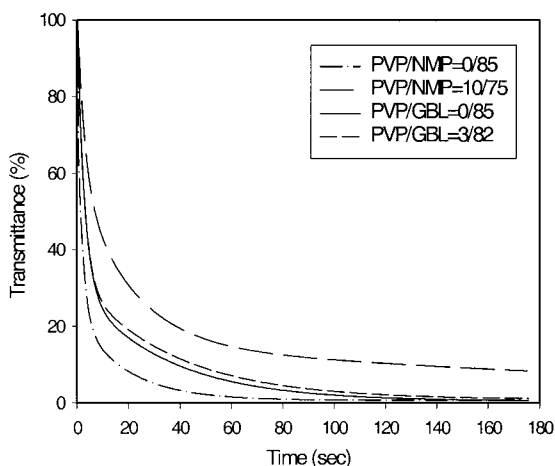


Figure 5 Effect of addition of PVP in 15 wt % PI solution on the light transmittance curve.

Table IV Degree of Shift in Real and Virtual Binodal Curves (DSVBC, DSRBC)

PVP (wt %)	DSVBC (%)		DSRBC ^a (%)	
	NMP System	DMF System	NMP System	DMF System
1	5.0	5.0	50.0	66.7
5	55.0	42.5	67.0	83.3
10	151.7	80.0	91.7	96.7

^a DSRBC in GBL system: 1 wt % PVP = 75.5%, 3 wt % PVP = 83.4%.

$$\text{DSBC} = \frac{\text{M.G. with no PVP} - \text{M.G. with PVP}}{\text{M.G. with no PVP}} \times 100 \quad (4)$$

where M.G. denotes the miscibility gap.

As shown in Table IV, DSVBC (degree of shift in virtual binodal curve) of the DMF system is smaller than that of the NMP system, whereas DSRBC (degree of shift in real binodal curve) of the DMF system is larger than that of the NMP system, which means more effective application of the virtual binodal in the NMP system than in the DMF system. Macrovoid formation in the NMP system, therefore, is more suppressed than that in the DMF system with addition of PVP. This can be comprehended by the fact that the application of virtual binodal theory is less effective, given the poorer solvency of DMF than NMP for PI and PVP.

In GBL and DMSO systems, the poor solvency of GBL and DMSO for two polymers promotes the polymer–polymer phase separation. The precipitation rate does not seem to be significantly affected by the addition of PVP in the GBL system, as shown in Figure 5. It could be comprehended by the fact that the content of PVP addition was rather small (3 wt %) and so the viscosity of the polymer solution did not increase extensively, compared with that of the NMP or DMF solution. In this case, the virtual binodal theory was not effectively adjusted because the polymer–polymer phase separation caused by poor solvency is predominant. Instead, the polymer–polymer phase separation weakens the resistance of polymer solution for macrovoid formation. The larger DSRBC in the GBL system establishes the easy tendency of polymer–polymer phase separation, as shown in Table IV.

Table V Effect of PVP on the Porosity of 15 wt % PI Membranes

PVP Content (%)	Overall Porosity ^a (%)			
	NMP System	DMF System	GBL System	DMSO System
0	77.2	74.0	53.1	73.0
1	77.2	74.3	58.2	73.9
3	78.9	76.5	72.7	nm
5	79.5	77.9	nm	nm
10	79.7	78.5	nm	nm

^a nm = not measurable because the miscibility gaps for PVP are 4 and 2% in PI/GBL and PI/DMSO solutions, respectively.

Overall Porosity

Although the effect of PVP on the membrane morphology was quite different, the result of overall porosity was consistent, irrespective of solvents used. That is, the overall porosity increased with the increasing content of PVP in PI solution, as represented in Table V. It should be noted that the PI/DMSO membrane without PVP possesses high porosity unlike that of the GBL system, in spite of the similar spongelike structure between the two systems. The differences of porosity between two systems may be the result of different membrane-formation mechanisms. The mechanism of membrane formation for the PI/DMSO/water system was described well in our previous study.¹⁵ The effect of PVP on the increase of the overall porosity was especially drastic in the GBL system. These results of overall porosity can be attributed to the soluble property of PVP in water, which leaches out of the membrane during precipitation. One may say that the larger content of PVP exists in the polymer-lean phase in the GBL system than in either the NMP or the DMF system. Therefore, the macrovoid formation in the GBL system becomes more vigorous.

CONCLUSIONS

In spite of the excellent miscibility of PI and PVP, the solubility gaps for PVP in PI solutions were varied, depending on the solvent used. This behavior could be explained by means of $\chi_{PI/Solvent}$ and $\Delta\delta_{PVP/Solvent}$. The large solubility gap for PVP in PI solution was produced mainly by low $\chi_{PI/Solvent}$ and low $\Delta\delta_{PVP/Solvent}$ and vice versa.

The effects of addition of PVP on the membrane morphology were varied, depending on the systems. In the NMP and DMF systems having high affinities of solvent/nonsolvent and polymer/solvent, fingerlike structures were inhibited with addition of PVP. On the other hand, macrovoid formation was promoted in the GBL and DMSO systems with addition of PVP. Suppression of fingerlike structure by addition of PVP into NMP and DMF systems would be explained by both the enlarged miscibility gap and increase of polymer solution viscosity. The decrease of macrovoids in the NMP system was particularly more drastic than that in the DMF system with the same amounts of PVP (10 wt %). This could be explained by the difference of DSBC in the two systems. Promotion of macrovoid formation in the GBL and DMSO systems may be explained by the reduced resistance for growth of pore formation caused by the polymer-polymer phase separation.

The overall porosity was increased with addition of PVP, irrespective of systems. When a small amount of PVP was added, however, the increases of overall porosity in the GBL system were more drastic than those in the NMP and DMF systems, implying that a larger amount of PVP remained in the polymer-lean phase in the GBL system than in the NMP and DMF systems.

The authors gratefully acknowledge partial support from the Creative Research Initiatives Program of the Korean Ministry of Science and Technology.

REFERENCES

- Loeb, S.; Sourirajan, S. *Adv Chem Ser* 1962, 38, 117.
- Reuvers, A. J.; Smolders, C. A. *J Membr Sci* 1987, 34, 67.
- Kang, Y. S.; Kim, H. J.; Kim, U. Y. *J Membr Sci* 1991, 60, 219.
- Boom, R. M.; Wienk, I. M.; Van den Boomgaard, T.; Smolders, C. A. *J Membr Sci* 1992, 73, 277.
- Kim, J. H.; Lee, K. H. *J Membr Sci* 1998, 138, 153.
- Huang, R. Y. M.; Feng, X. *J Appl Polym Sci* 1995, 57, 613.
- Wang, D. M.; Lin, F. C.; Wu, T. T.; Lai, J. Y. *J Membr Sci* 1998, 142, 191.
- Lai, J. Y.; Lin, F. C.; Wang, C. C.; Wang, D. M. *J Membr Sci* 1996, 118, 49.
- Kang, Y. S.; Jung, B.; Kim, U. Y. *U.S. Pat.* 5,795,920, 1998.

10. Won, J.; Kang, Y. S.; Park, H. C.; Kim, U. Y. *J Membr Sci* 1998, 145, 45.
11. Kang, Y. S.; Kim, J.; Rhee, H.-W.; Jung, B.; Park, H. C.; Won, J.; Kim, U. Y. *Korea Polym J* 1997, 5, 166.
12. Smolders, C. A.; Reuvers, A. J.; Boom, R. M.; Wienk, I. M. *J Membr Sci* 1992, 73, 259.
13. Van Krevelen, D. W. *Properties of Polymers*; Elsevier: Amsterdam, 1990.
14. Durant, Y. G.; Sundberg, D. C.; Guillot, J. *J Appl Polym Sci* 1994, 52, 1823.
15. Kim, J. H.; Min, B. R.; Won, J.; Park, H. C.; Kang, Y. S. *J Membr Sci* 2001, 187, 47.
16. Roesink, H. D. W. Ph.D. Thesis, University of Twente, The Netherlands, 1989.
17. Gomez, C. M.; Verdejo, E.; Figueruelo, J. E.; Campos, A.; Soria, V. *Polymer* 1995, 36, 1487.
18. Zeman, L.; Tkacik, G. *J Membr Sci* 1988, 36, 119.
19. Yilmaz, L.; Mchugh, A. J. *J Appl Polym Sci* 1986, 31, 997.
20. Boom, R. M.; Reinders, H. W.; Rolevink, H. H. W.; Van den Boomgaard, T.; Smolders, C. A. *Macromolecules* 1994, 27, 2041.
21. Boom, R. M.; Van den Boomgaard, T.; Smolders, C. A. *J Membr Sci* 1994, 90, 231.
22. Yanagishita, H.; Nakane, T.; Yoshitome, H. *J Membr Sci* 1994, 89, 215.
23. Frommer, M. A.; Messalem, R. M. *Ind Eng Chem Prod Res Dev* 1973, 12, 328.